Operando IR and Raman Spectroscopy of the Catalyst Ionomer Interface

Neili Loupe[a], Jonathan Doan[a], Ryan Cruse[a], Nicholas Dimakis[b], Khaldoon Abu-Hakmeh[c], Seung Soon Jang[c], William A Goddard III[d], Eugene S. Smotkin[a]

a: Department of Chemistry and Chemical Biology
Northeastern University
Boston, MA 02115
e.smotkin@neu.edu

b: Department of Physics
University of Texas Rio Grande Valley
Edinburg, TX 78539

c: School of Materials Science and Engineering
Georgia Institute of Technology
Atlanta, GA 30332

d: Materials and Process Simulation Cente
California Institute of Technology
Pasadena, CA 91125

DOE Catalysis Working Group Meeting
Argonne National Laboratory, Building 241/D172
Wednesday, July 27. 2016

Overview

1. Operando spectroscopy fuel cells (IR, XAS, Raman)
2. Why operando?
   - Structural changes during catalysis (XAS case study)
3. IR spectroscopy of catalyst ionomer interface
   - Molecular orbital explanation of CO_{ads} Stark tuning
   - Stark tuning: Probe for interfacial co-adsorption and electrocatalysis
4. IR spectroscopy in proximity to the catalyst/ionomer interface
   - Short chain, 3M and Nafion membranes
     - Band assignments in terms of exchange site local symmetry
     - C_1 (sulfonic acid) and C_{3V} (sulfonate) local symmetry modes
     - Hydration dependent distribution of per site λ (waters/exchange site).
       - Molecular dynamics modeling and state of hydration IR spectroscopy
5. Fuel cell operando Raman spectroscopy (Case study: Non-PGM catalyst)
   - Membrane exchange site transition from C_1 to C_{3V} symmetry during ORR
   - No Stark tuning of Fe-O stretching mode
   - Catalysis hypothesized as due to 14 ppm Pt contaminant

Operando IR and Raman spectroscopy

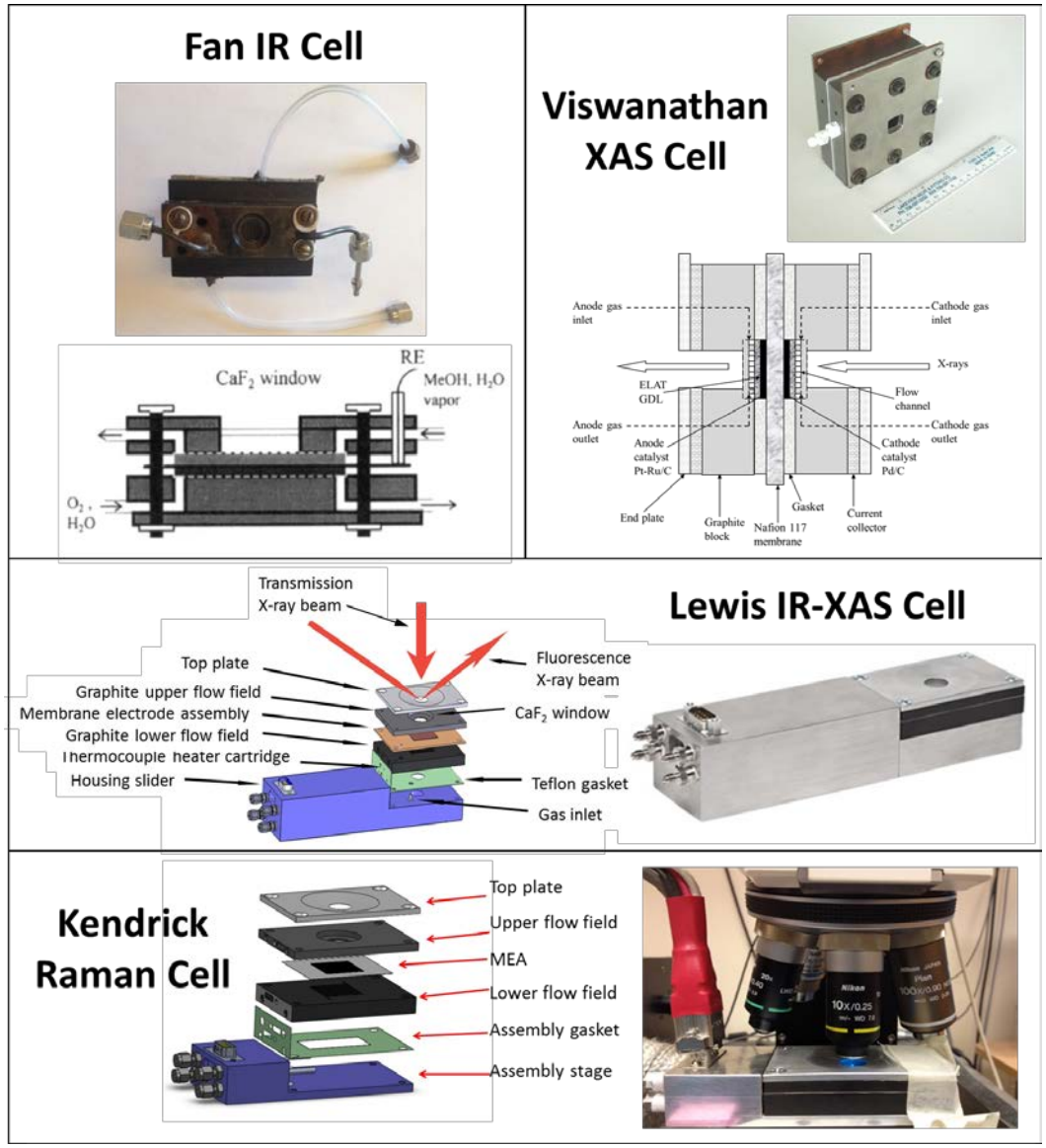

Operando direct methanol fuel cell X-ray absorption spectroscopy: A case study exemplifying the need for operando measurements.

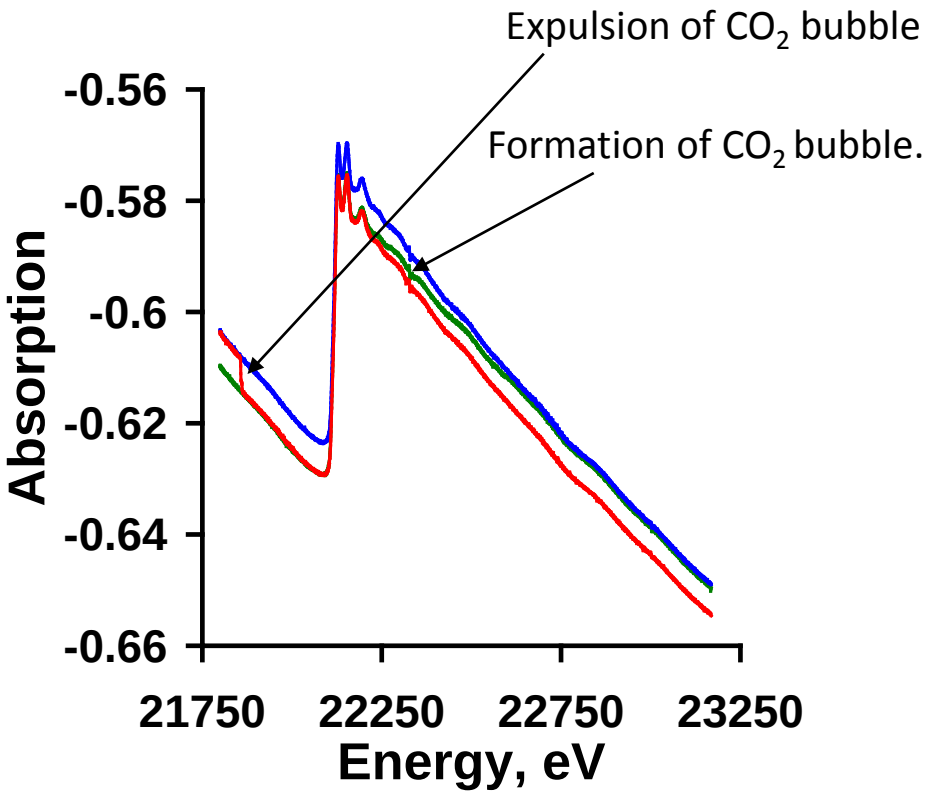

CO_2 phase-out was mitigated by application of a backpressure to the methanol anode.

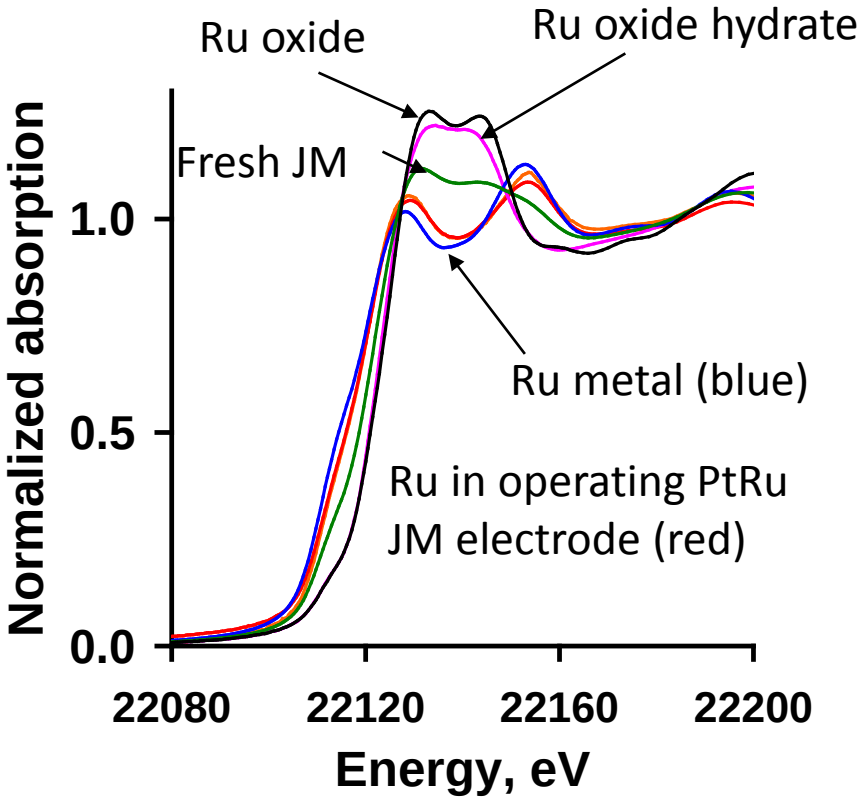

Operando DMFC anode is always metallic

S Stoupin et al. *Pt and Ru X-ray Absorption Spectroscopy of PtRu Anode Catalysts in Operating Direct Methanol Fuel Cells* J Phys Chem B, 110, 9932 -9938, **(2006)**

Johnson Matthey PtRu (1:1) structural changes during catalysis

As received PtRu (1:1)

- Ru oxidation ~58%
- N = 5.6
- [Ru]/[Pt] = 0.44
- Pt-O bonds present
- Ru-O bonds ~2.8 avg

Operando PtRu (1:1)

- Ru oxidation ~15%
- N = 8.2
- [Ru]/[Pt] = 0.50
- No Pt-O bonds
- Ru-O bonds ~0.24 avg

S Stoupin et al., J.Phys Chem B, **110**, 9932 (2006).

Vibrational Spectroscopy of the Pt/ionomer interface

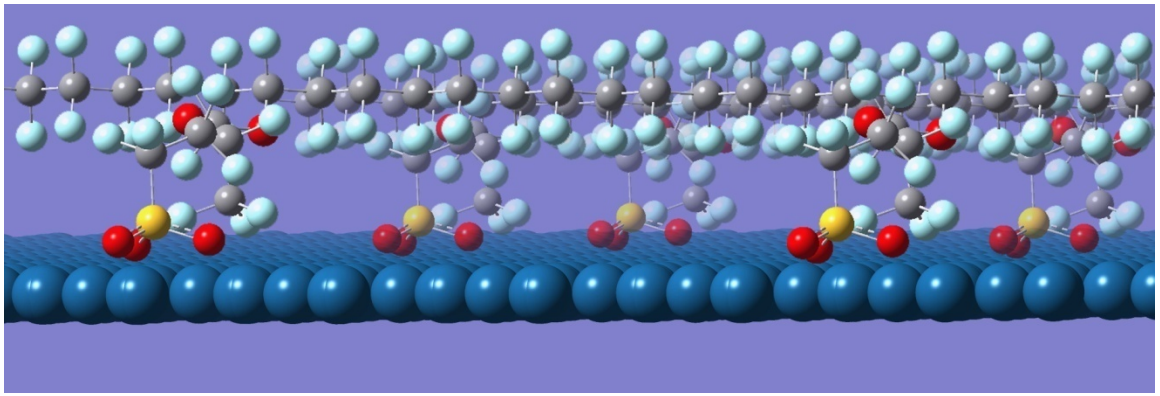

Co-adsorbates include sulfonate exchange site and the $-CF_3$ group.

I Kendrick et al. *Elucidating the Ionomer-Electrified Metal Interface*, J. Am. Chem. Soc., 132 (49), 17611–17616 (2010**)**

Stark Tuning: Potential dependent CO_{ads} stretching frequencies.
Higher electrode Fermi levels = Reduced CO stretching frequencies.

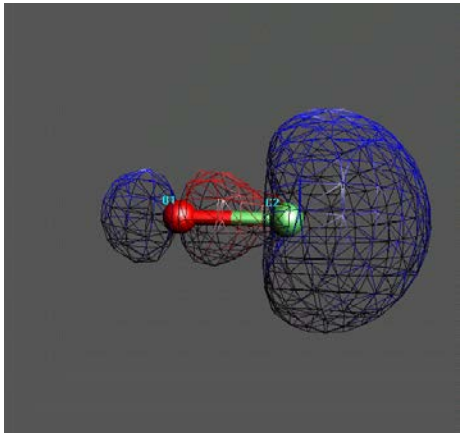

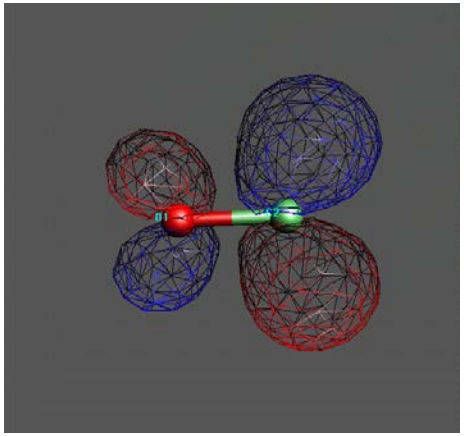

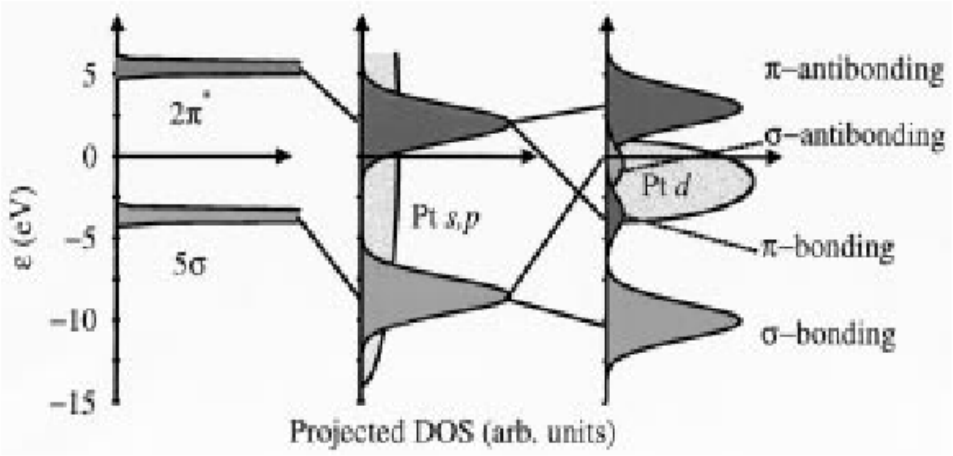

B. Hammer, O. H. Nielsen and J. K. Norskov, *Catalysis Letters*, 1997, **46**, 31-35

Stark tuning: From model surfaces to fuel cell Pt/ionomer interfaces

Model surfaces

R Liu et al. *Potential-Dependent Infrared Absorption Spectroscopy of Adsorbed CO and X-ray Photoelectron Spectroscopy of Arc-Melted Single-Phase Pt, PtRu, PtOs, PtRuOs, and Ru Electrodes*, J. Phys. Chem. B, 104 (15), 3518–3531 (2000)

V Stamenkovic et al. *Vibrational Properties of CO at the Pt(111)−Solution Interface: the Anomalous Stark-Tuning Slope*, JPC B, *109*, 678-680 (2005)

MEA Catalyst ionomer interfaces

I Kendrick et al. *Elucidating the Ionomer-Electrified Metal Interface*, J. Am. Chem. Soc., *132* (49), 17611–17616 (2010)

S E Evarts et al. *Ensemble Site Requirements for Oxidative Adsorption of Methanol and Ethanol on Pt Membrane Electrode Assemblies*, ACS Catalysis, *2*, 701 (2012)

I Kendrick et al. *Operando Infrared Spectroscopy of the Fuel Cell Membrane Electrode Assembly Nafion-Platinum Interface*, International Journal of Hydrogen Energy, *39, 6, 2751-2755 (*2014)

CO_{ads} Stark tuning on Pt/Nafion interfaces

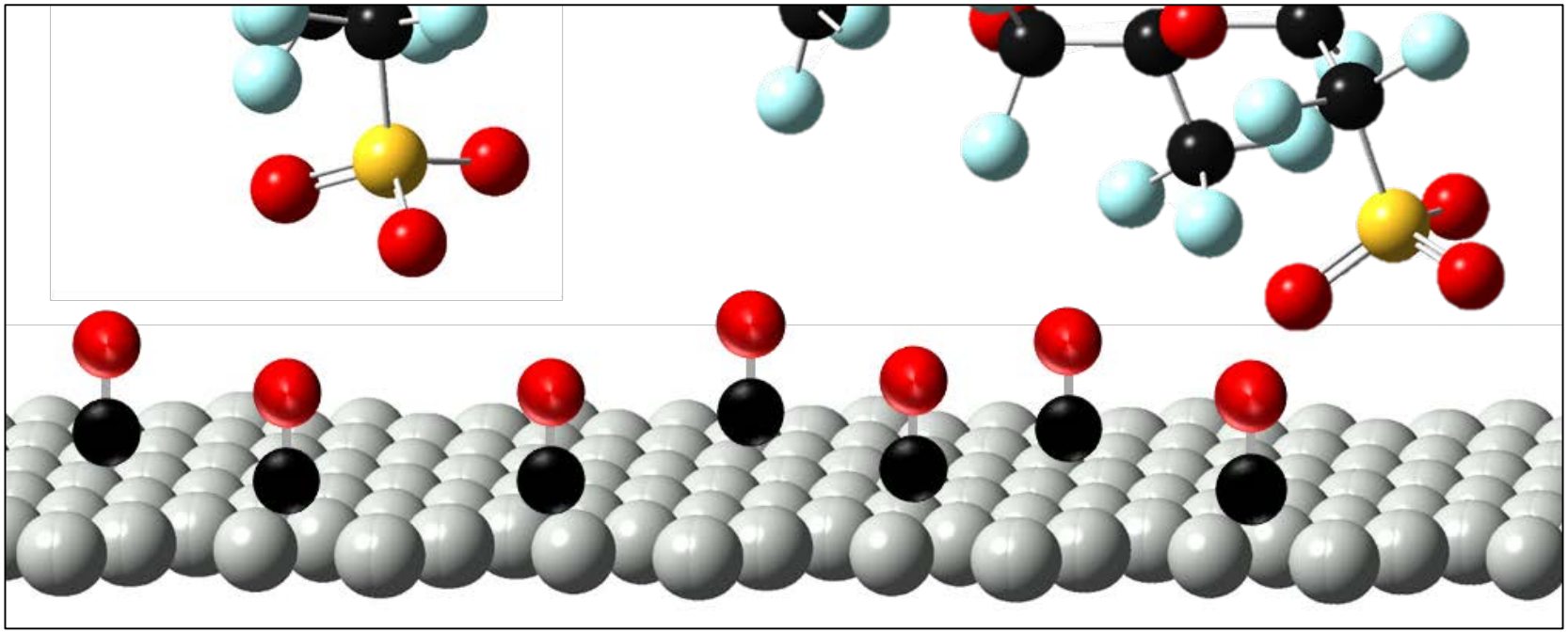

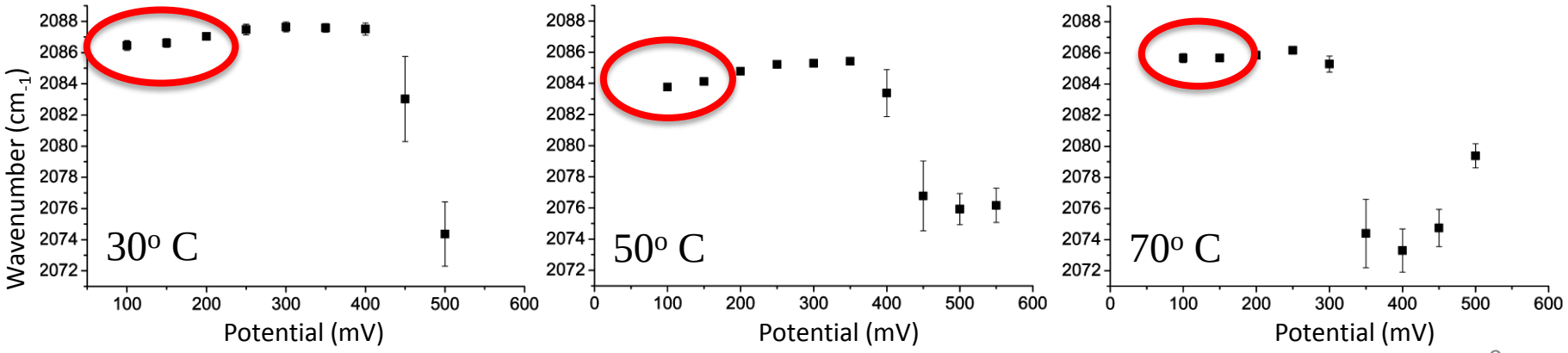

Operando Stark tuning at MEA Pt-CO_{ads} /Nafion interfaces

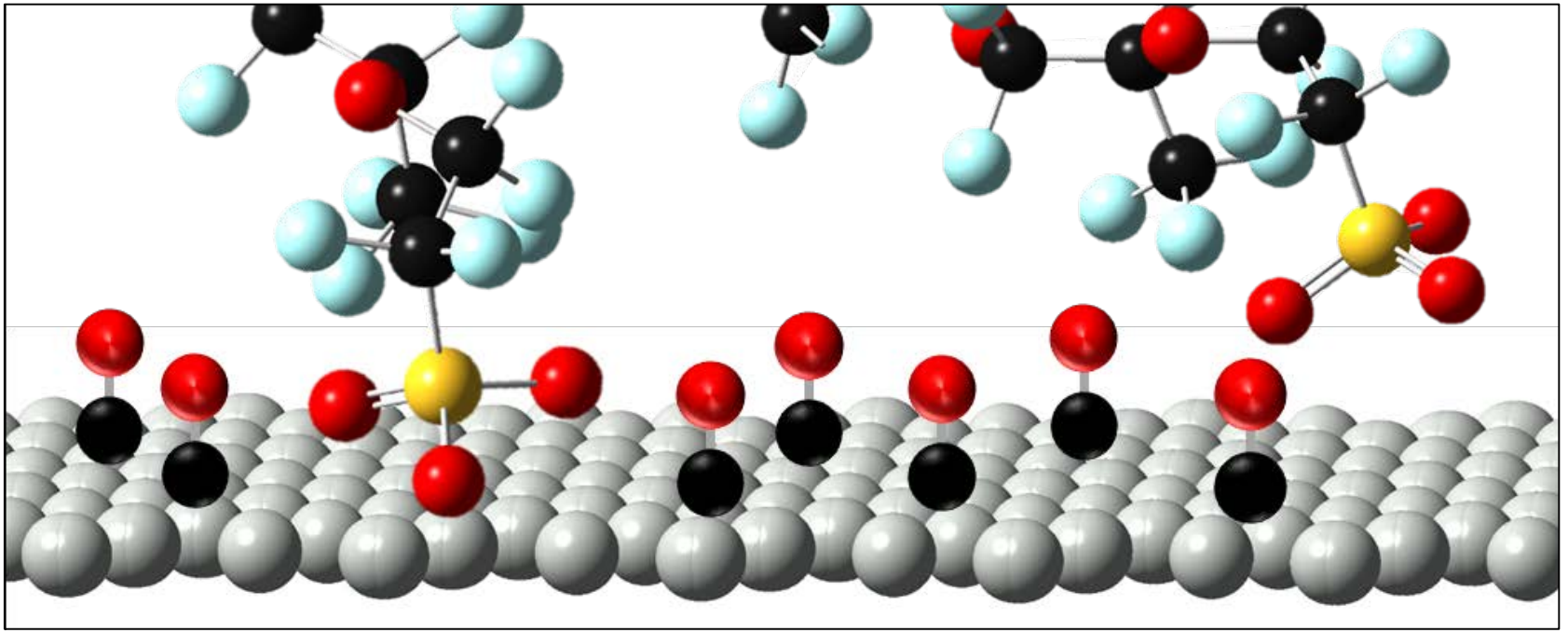

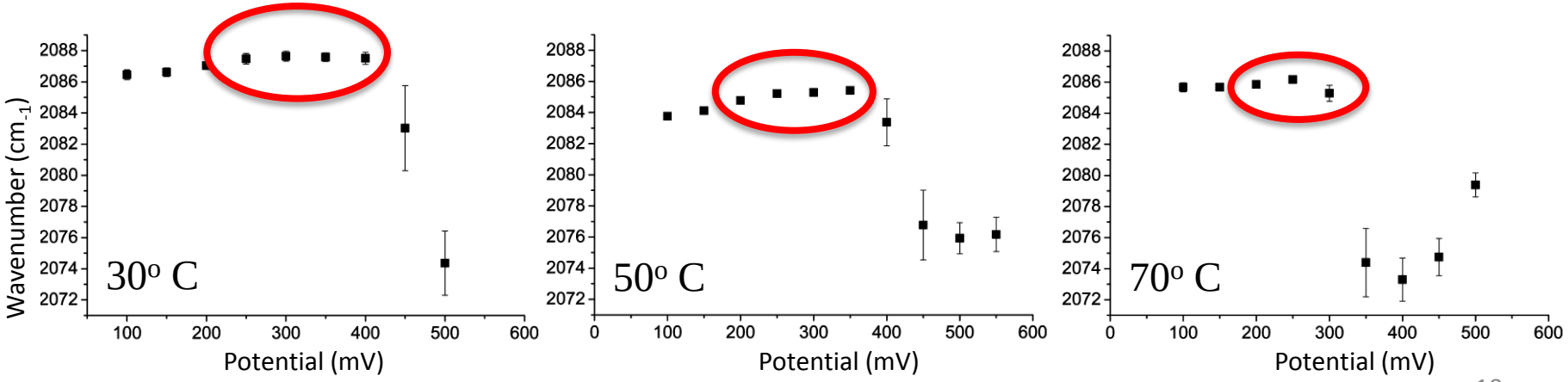

Operando Stark tuning at MEA Pt-CO_{ads} /Nafion interfaces

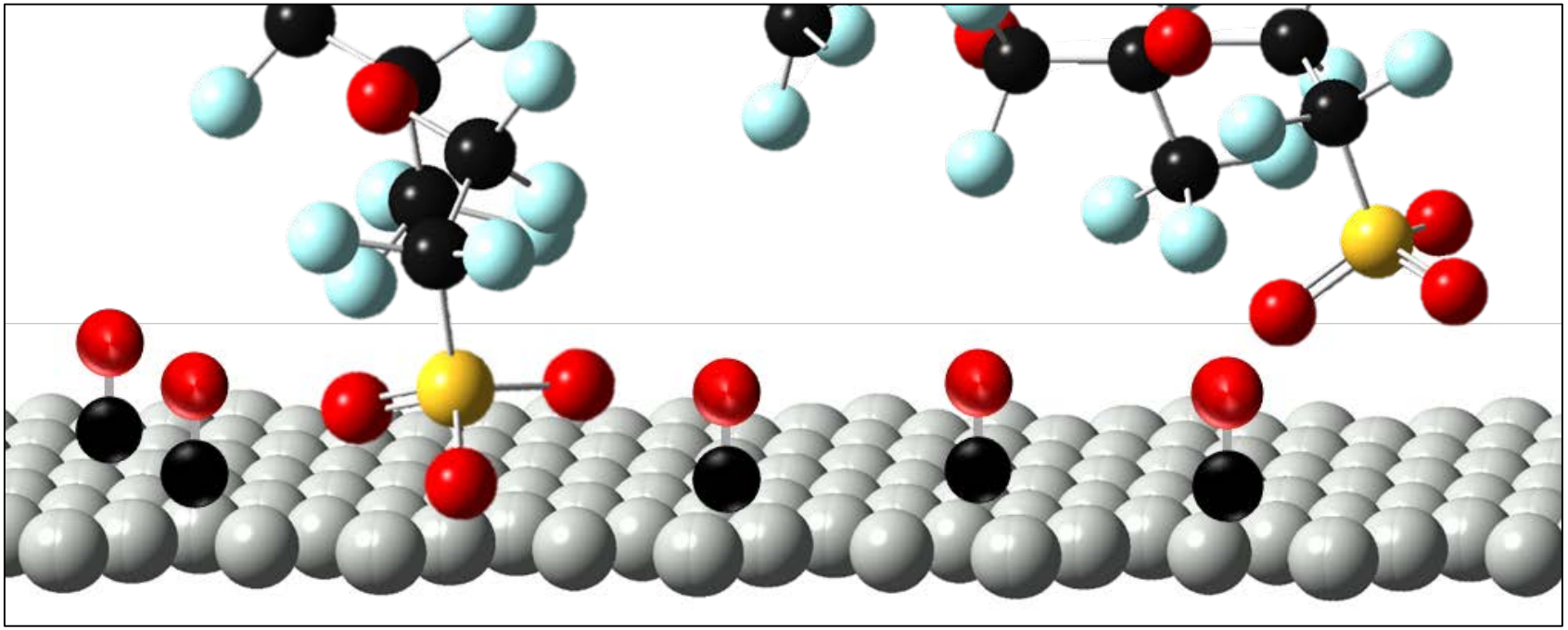

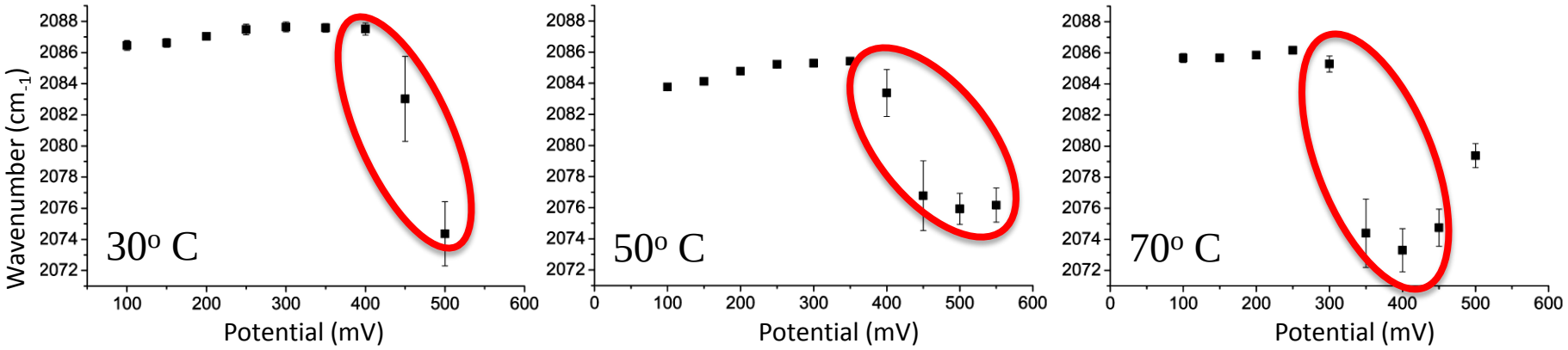

Operando Stark tuning at MEA Pt-CO_{ads} /Nafion interfaces

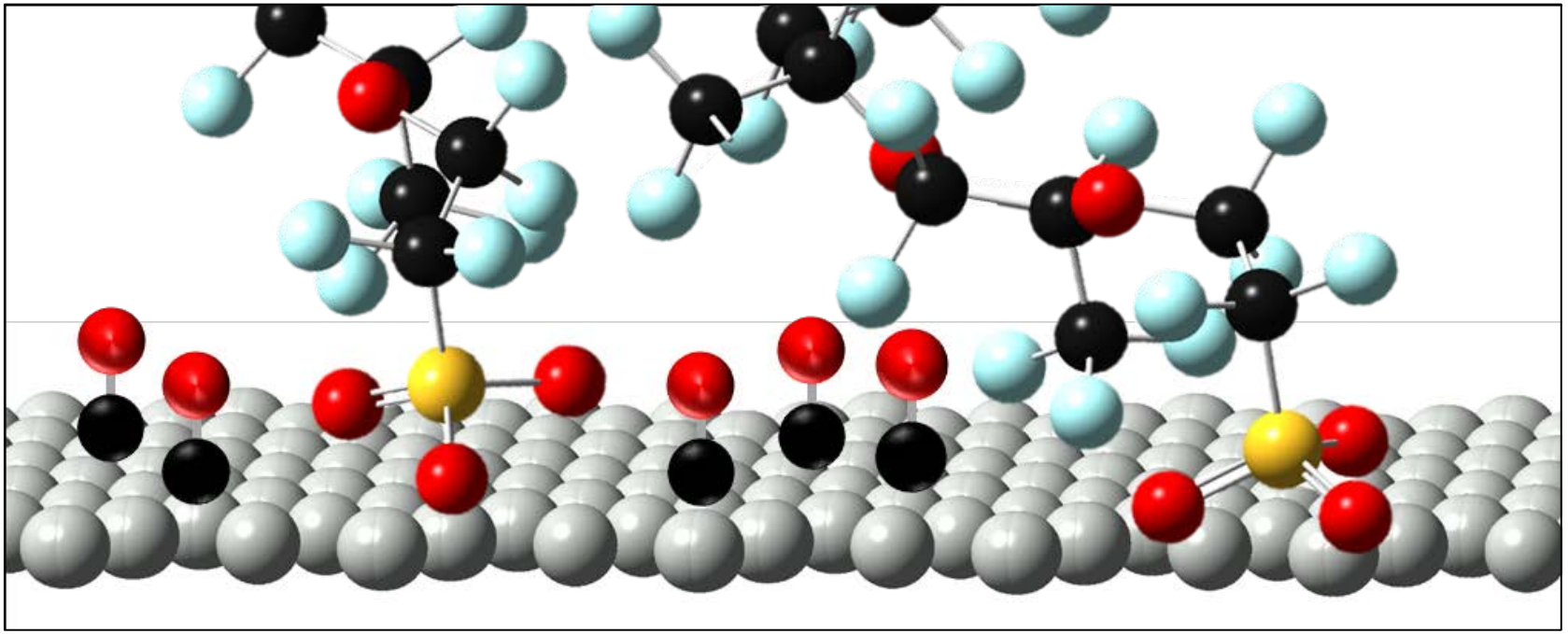

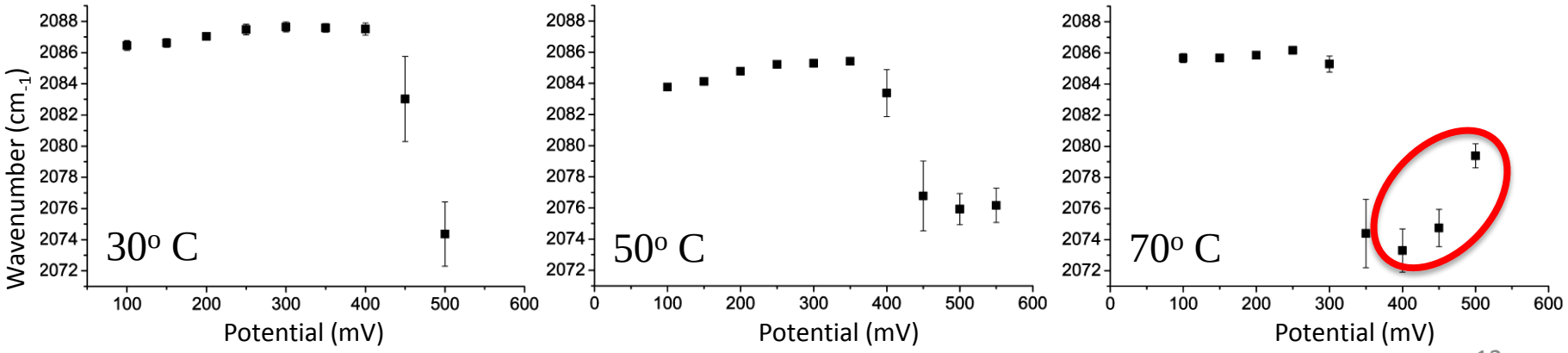

Operando CO_{ads} Stark tuning elucidates site specific (potential dependent) adsorption sites.

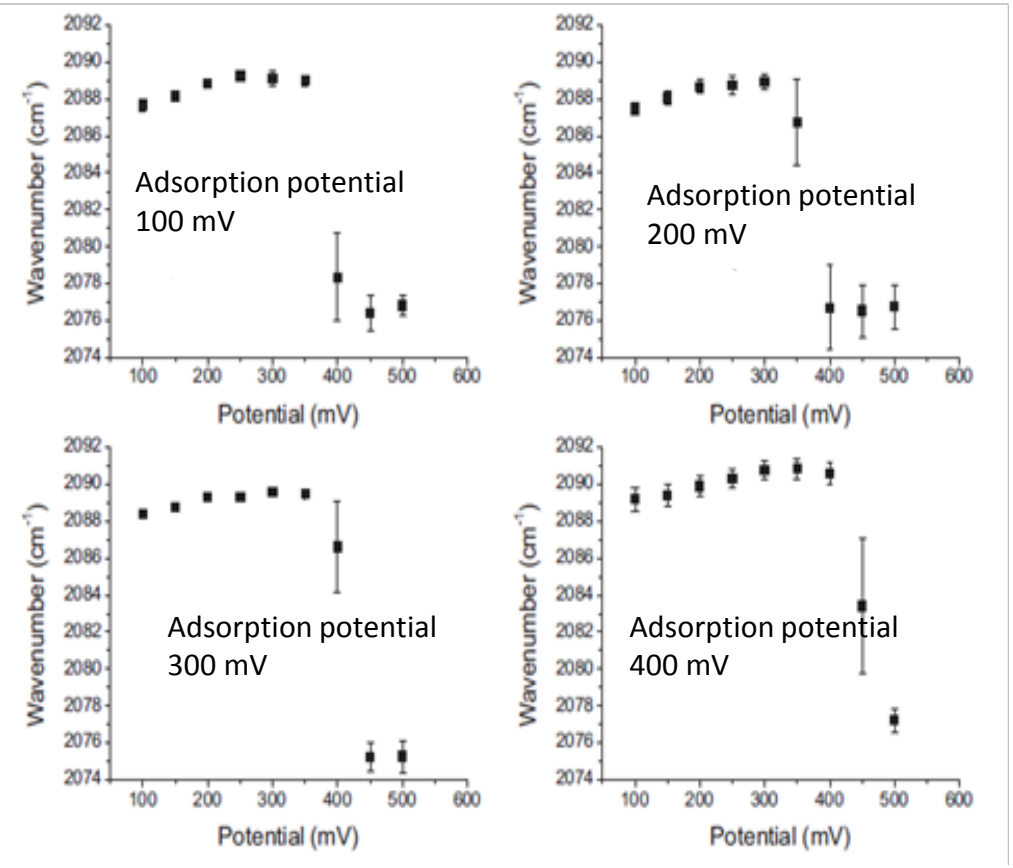

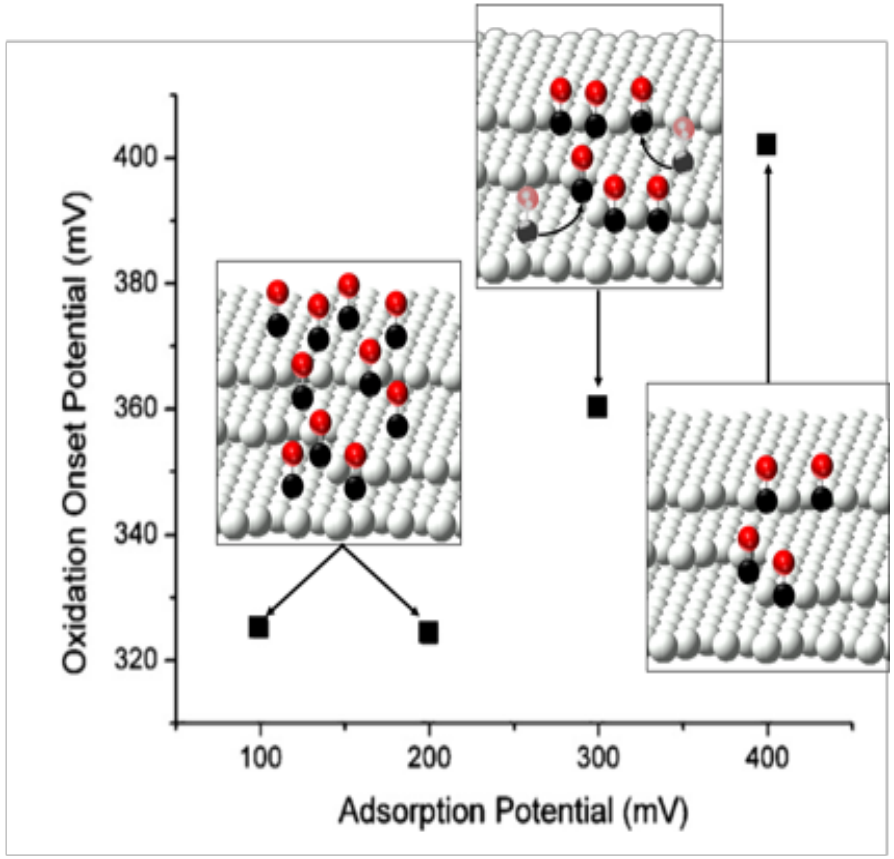

Hydration dependent IR spectra: Short chain, Nafion & 3M membranes

Short Side Chain

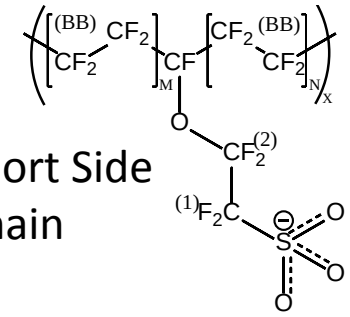

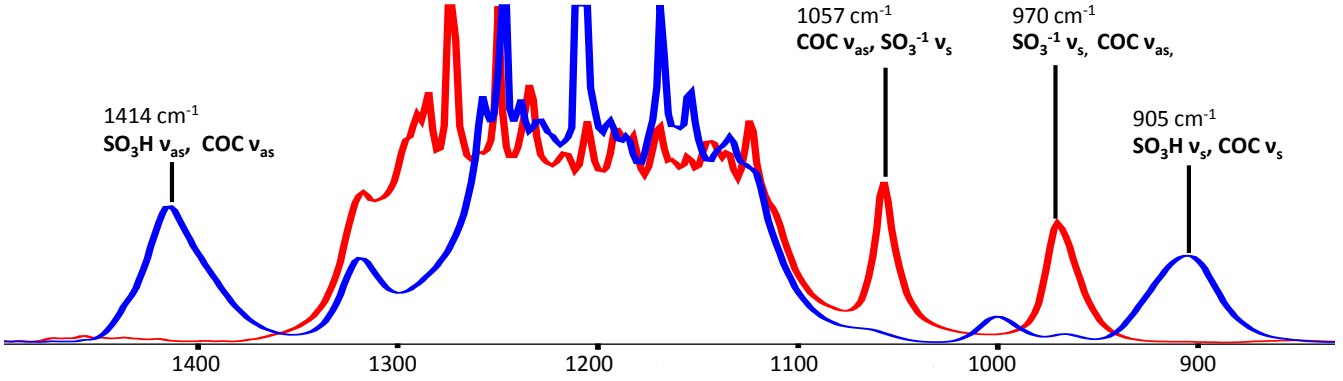

Nafion

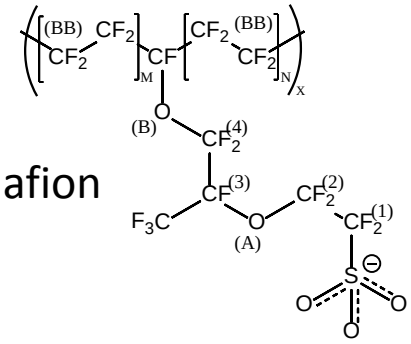

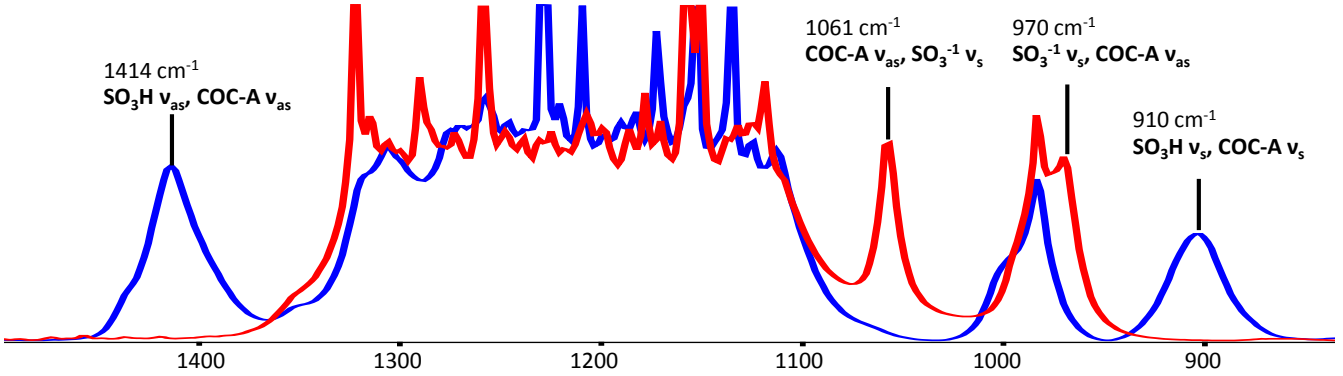

3M

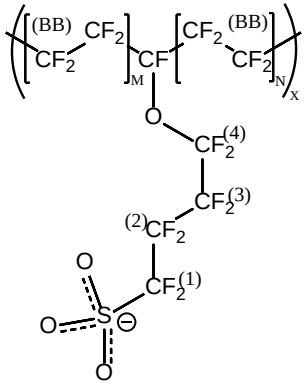

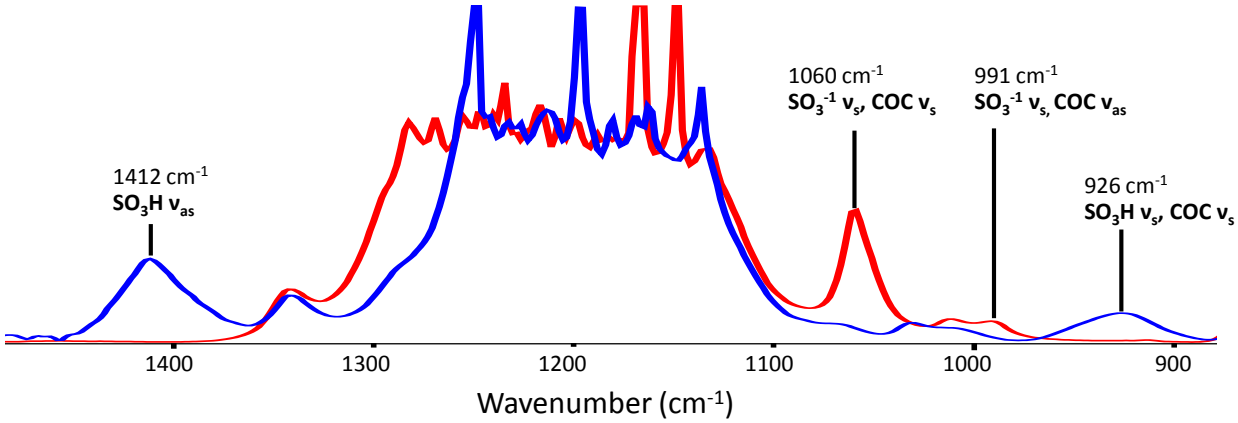

Nafion exchange-site normal mode animations

C_{3v} local symmetry

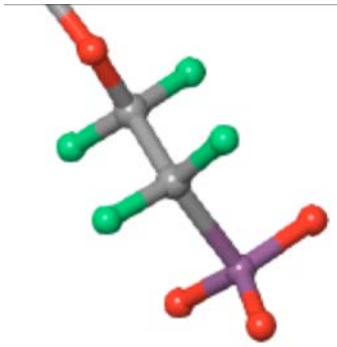

$C_{3v,LF}$

983* (969) cm^{-1} : SO_3^- v_s, COC-A v_{as}

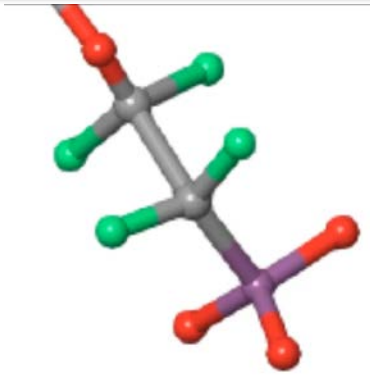

$C_{3v,HF}$

1059* (1061) cm^{-1} : COC-A v_{as}, SO_3^- v_s

C_1 local symmetry

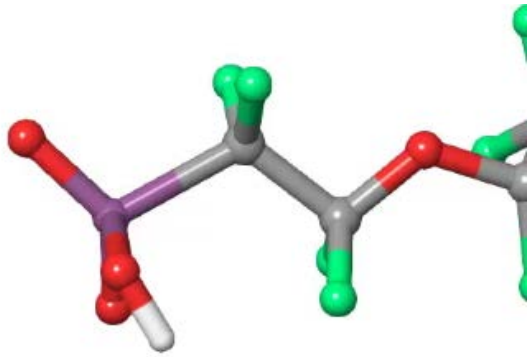

$C_{1,LF}$

786* (910) cm^{-1} : SO_3H v_s, COC-A v_s

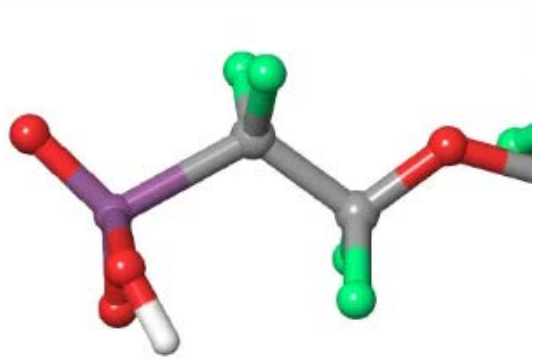

$C_{1,HF}$

1405* (1414) cm^{-1} : SO_3H v_{as}, COC-A v_{as}

Kendrick, I.; Yakaboski, A.; Kingston, E.; Doan, J.; Dimakis, N.; Smotkin, E. S. *J. Polym. Sci. Pt. B-Polym. Phys.* **2013**, *51*, 1329.

Normal mode animation snapshots (C_{3V}): Dissociated exchange sites.

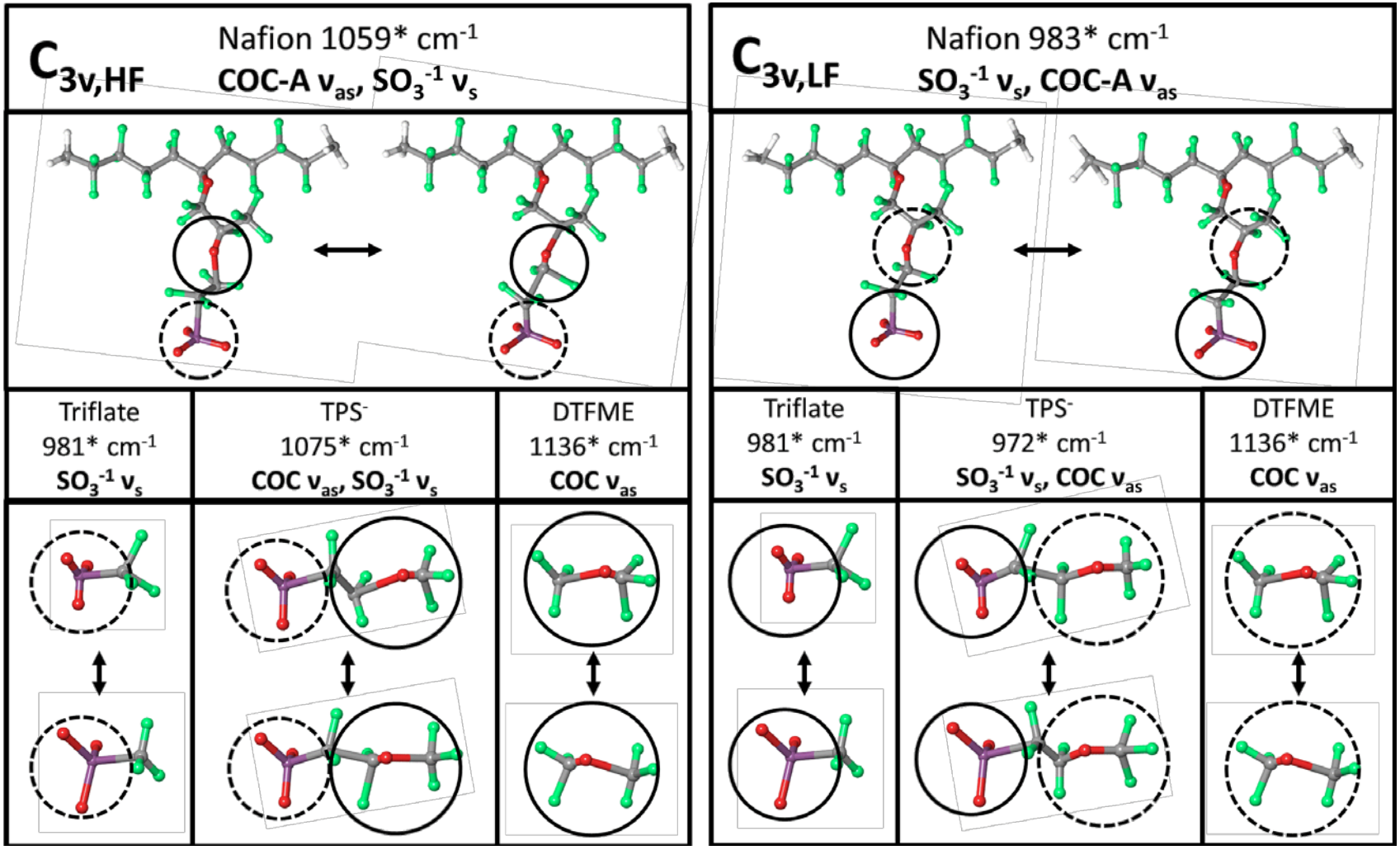

Kendrick, I., et al., *Operando Raman Micro-Spectroscopy of Polymer Electrolyte Fuel Cells.* Journal of The Electrochemical Society, 2016. **163**(4): p. H3152-H3159.

Normal mode animation snapshots (C_1): Associated exchange sites.

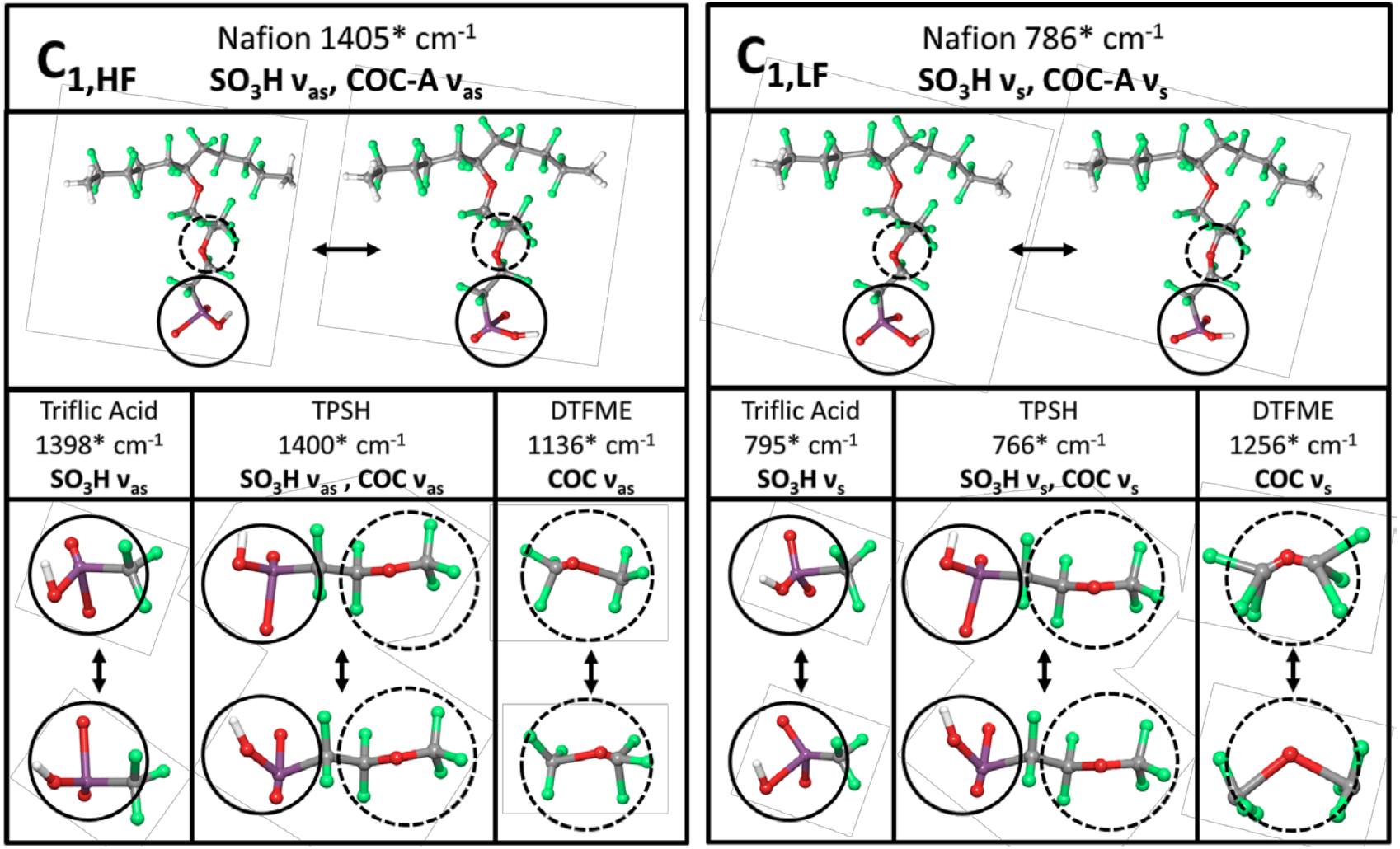

Kendrick, I., et al., *Operando Raman Micro-Spectroscopy of Polymer Electrolyte Fuel Cells.* Journal of The Electrochemical Society, 2016. **163**(4): p. H3152-H3159.

Operando spectroscopy: Transitioning between hydration (C_{3V}) and dehydration (C_1).

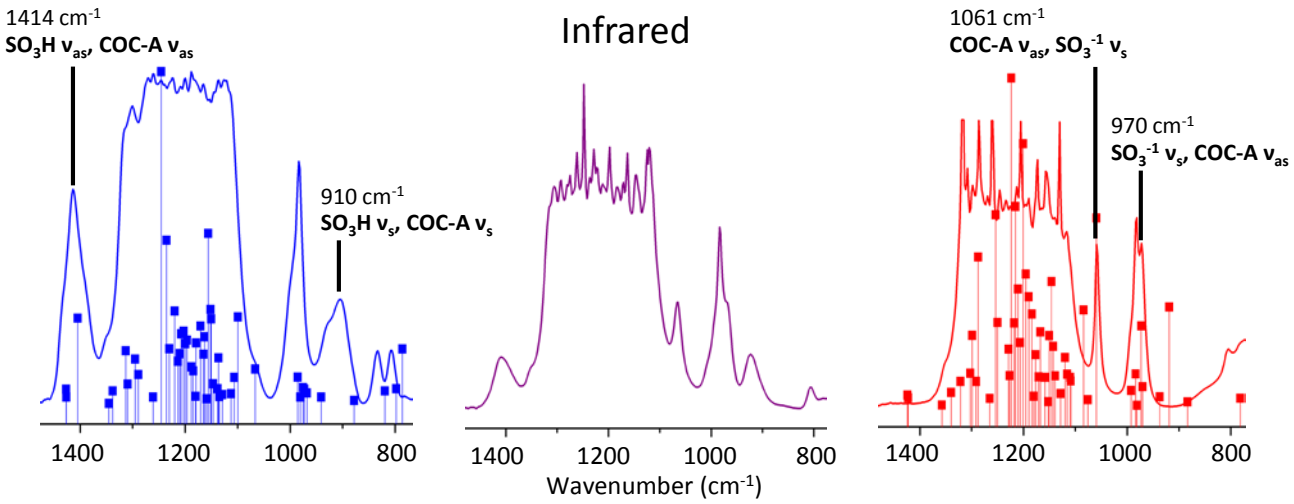

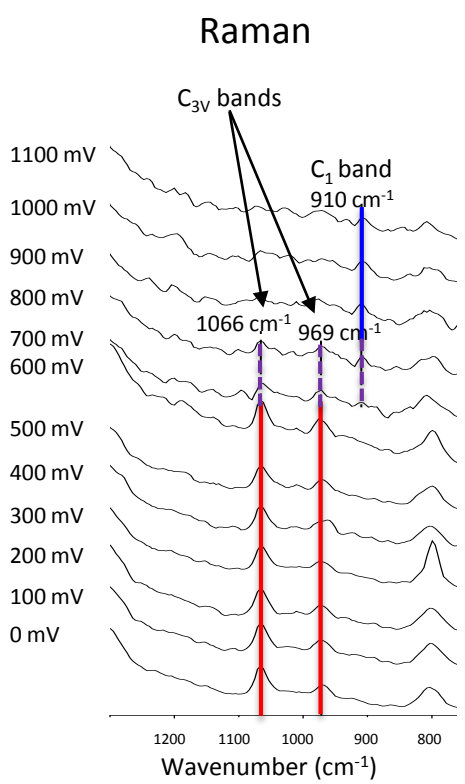

Dehydrated ⟷ Hydrated

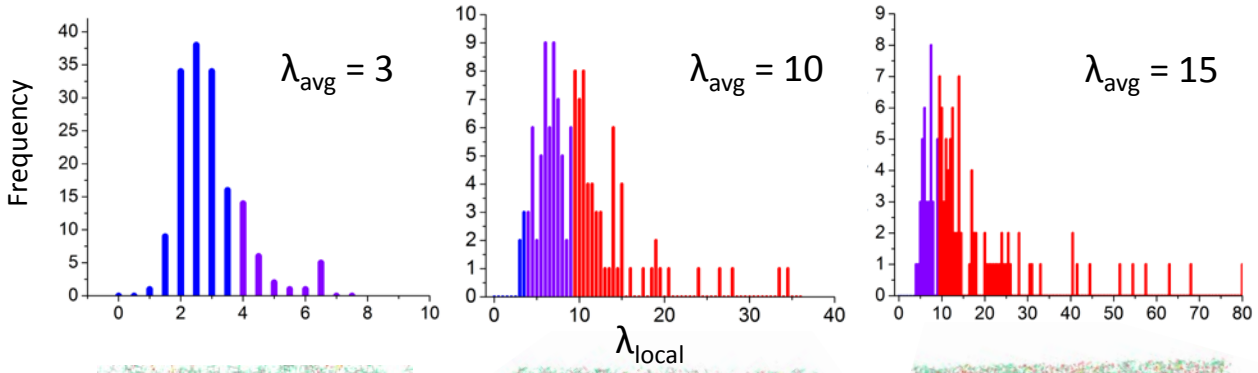

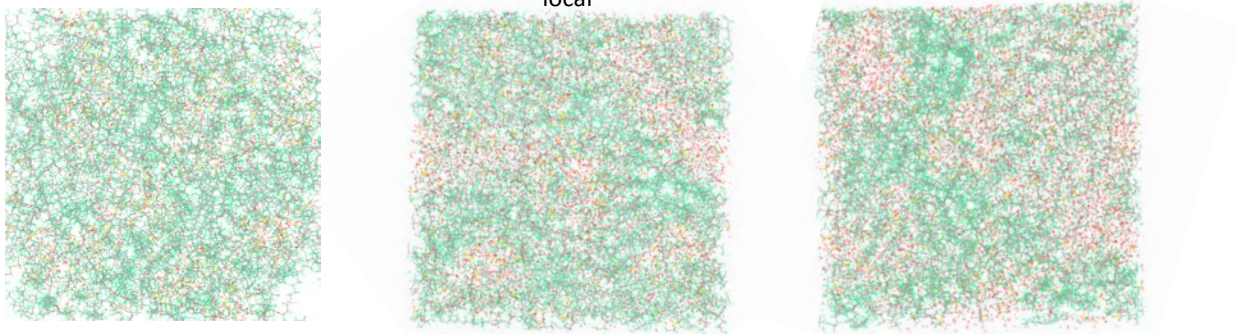

EW ~ 1100 g
32 oligomers
10 side chains separated by 14 - CF_2- monomers
320 exchange sites

Nafion dehydration: C_1 modes negatively correlated to C_{3V} modes.

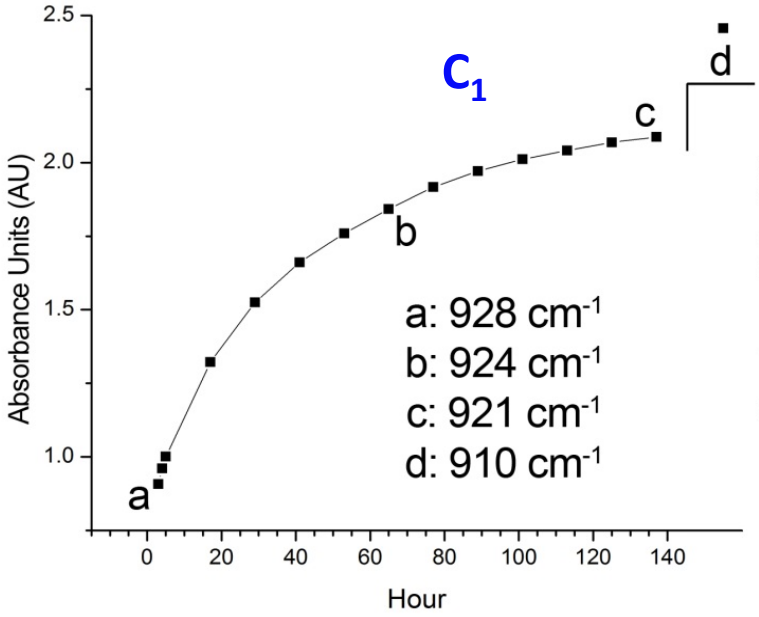

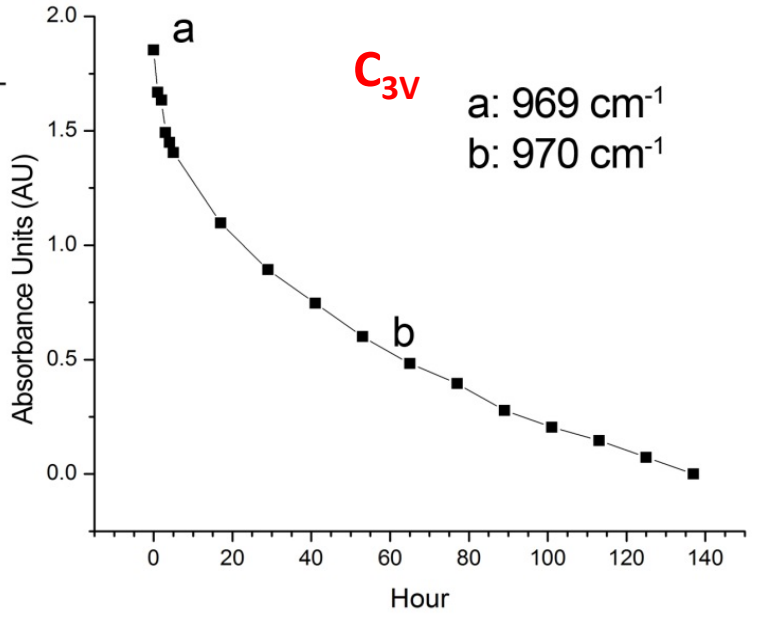

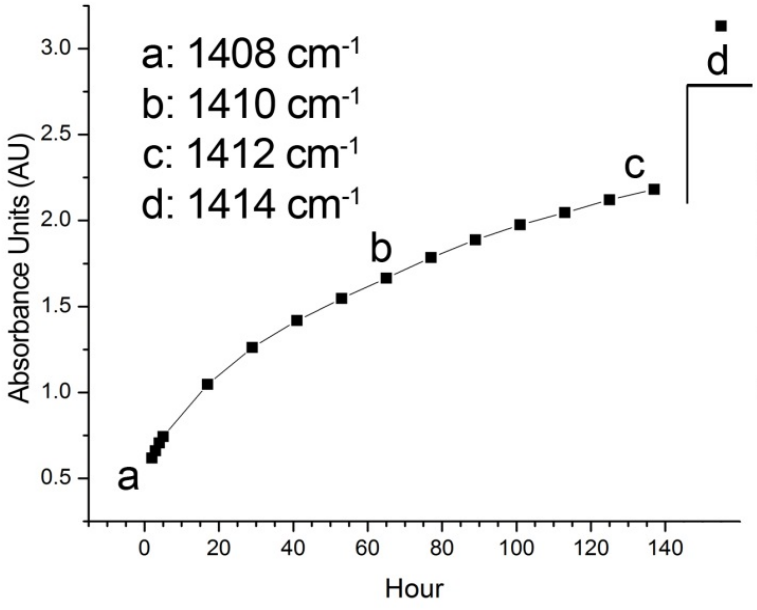

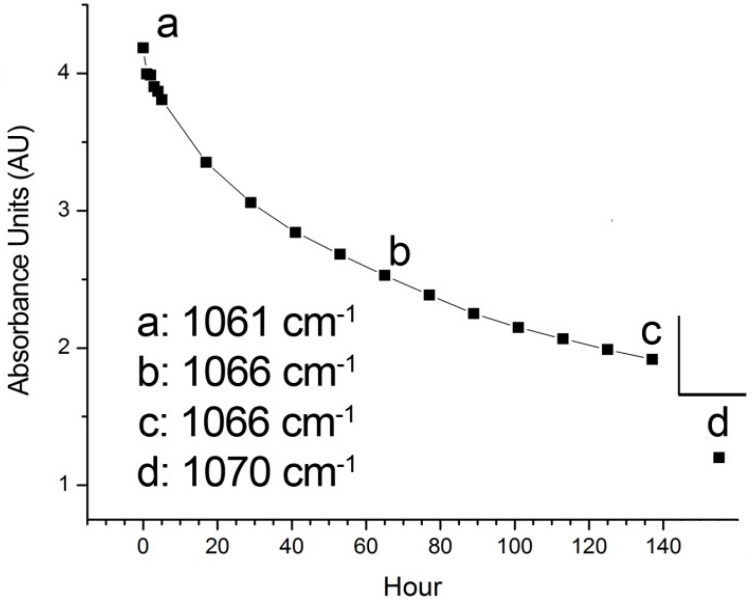

DFT build-up of the exchange site solvation sphere. Transitioning from C_1 to C_{3V} local symmetry

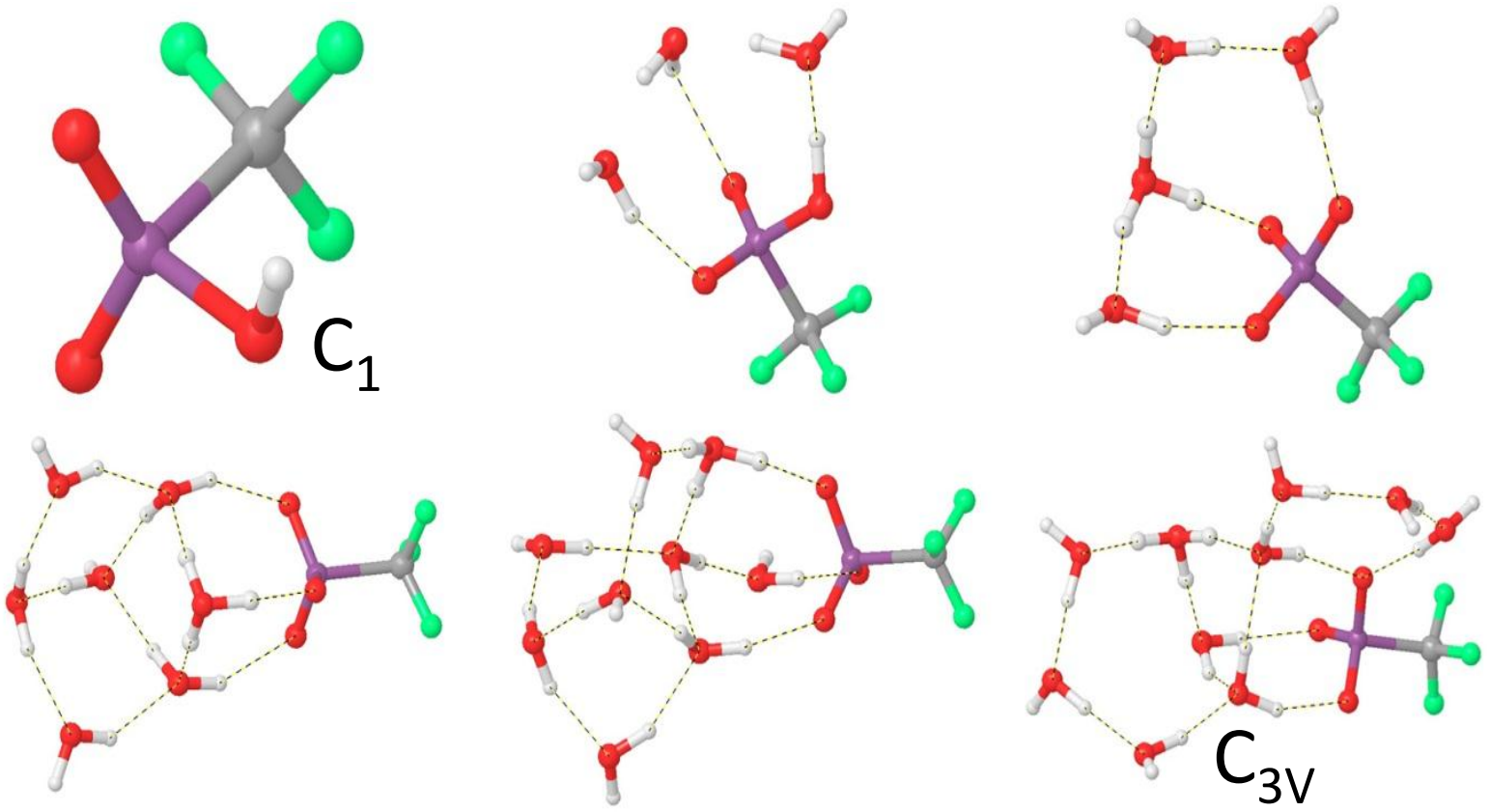

Webber et al. *Mechanically Coupled Internal Coordinates of Ionomer Vibrational Modes*, Macromolecules, 43, 5500-5502 (2010)
Kendrick et al. *Theoretical and experimental infrared spectra of hydrated and dehydrated Nafion* Journal of Polymer Science Part B: Polymer Physics, 51, 18, pp. 1329–1334 (2013)

Nafion Molecular Dynamics

- An initial cubic MD box was constructed with side lengths of ~80 Å (shrank to **75 Å**, during preliminary relaxation process)
- (Nafion with ~20 wt % (H_2O, H_3O^+)
  - Nafion EWs close to 1100 g/mol
    - 32 independent oligomers 10 side chains separated by 14 - CF_2- monomers
  - **4800 H_2O molecules**
  - **320 H_3O^+ ions**
- MD contained total **37,504 atoms**.
- Effective level of hydration **λ= 15**.

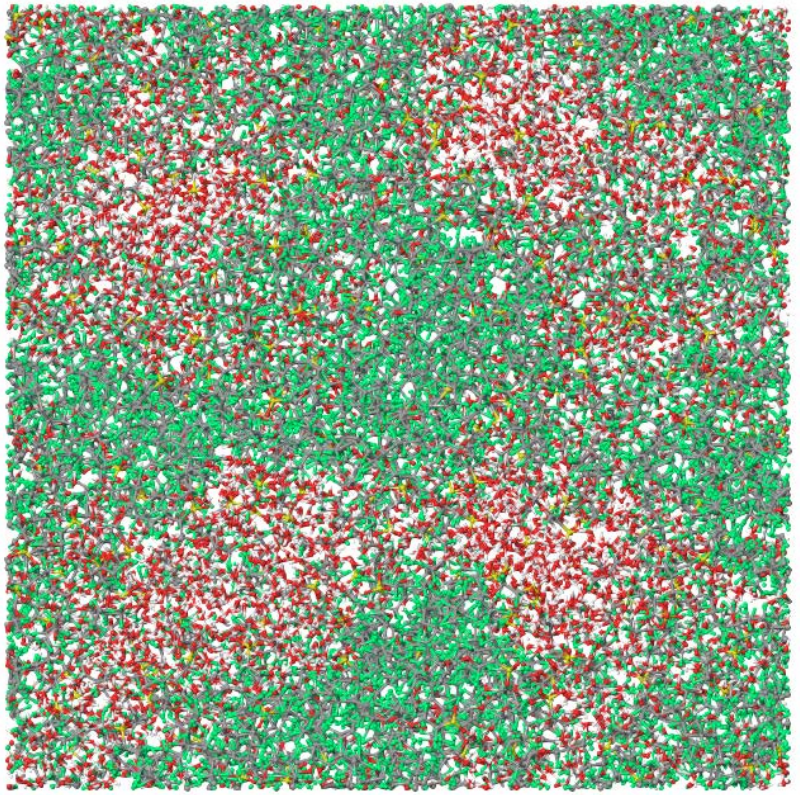

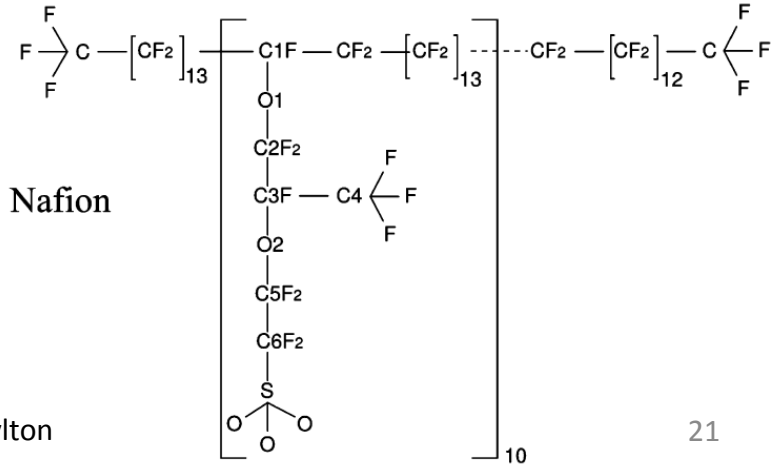

Karo, J., et al., Molecular Dynamics Modeling of Proton Transport in Nation and Hylton Nanostructures. Journal of Physical Chemistry B, 2010. 114(18): p. 6056-6064.

Nafion molecular dynamics: At any λ_{ave} a λ distribution exists.

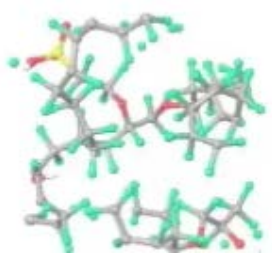

λ_{local} =0

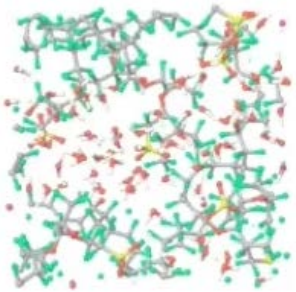

λ_{local} =10

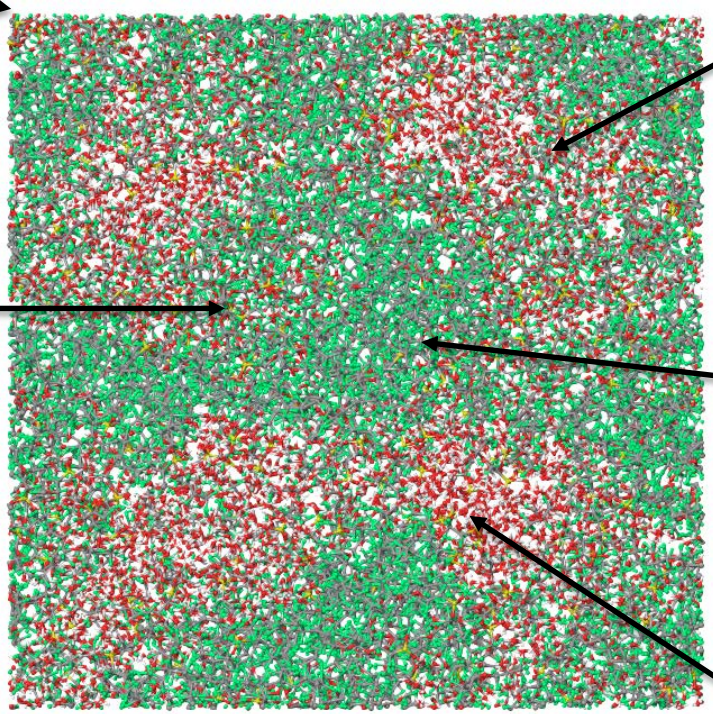

λ_{avg} =15

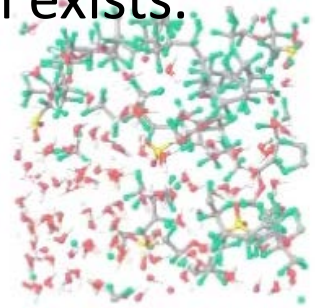

λ_{local} =15

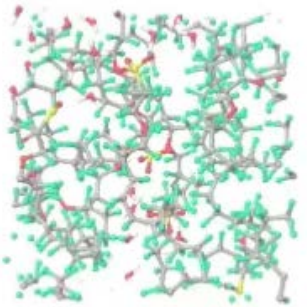

λ_{local} =4

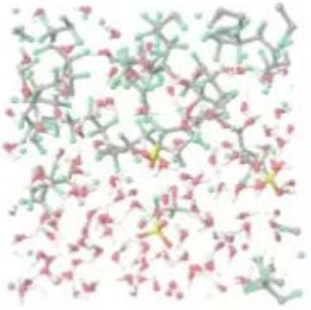

λ_{local} =40

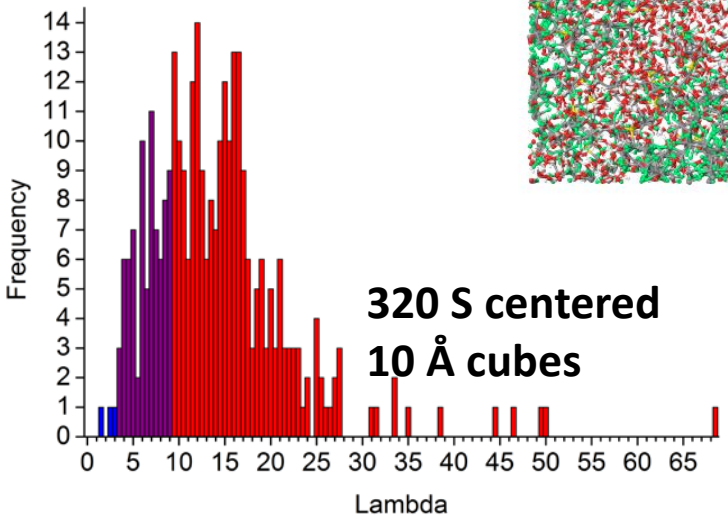

320 S centered
10 Å cubes

Nafion hydration (C_{3V})/dehydration (C_1) of the exchange site environment

- The C_1 and C_{3V} group modes involve the same side-chain functional groups (Triflate/COC group modes (C_{3V}) or triflic acid/COC group modes (C_1)).

- The C_1 and C_{3V} modes do not coexist at extreme states of hydration.

- C_1 and C_{3V} modes do coexist at intermediate state-of-hydration and there is a distribution of per site λ values.

IR band assignments of short chain, 3M and Nafion in terms of exchange site local symmetry (manuscript in preparation).

	Local symmetry	Group Mode Assignment	DFT (cm^{-1})	Transmission (cm^{-1})
Hydrated DOW-[H]	$C_{3v,LF}$	SO_3^{-1} ν_s, COC ν_{as},	923*	970
	$C_{3v,HF}$	COC ν_{as}, SO_3^{-1} ν_s	1051*	1057
Dehydrated DOW-[H]	$C_{1,LF}$	SO_3H ν_s, COC ν_s	777*	905
	$C_{1,MF}$	COC ν_s , SO_3H ν_{as}	960*	1001
	$C_{1,HF}$	SO_3H ν_{as}, COC ν_{as}	1396*	1414
Hydrated Nafion-[H]	$C_{3v,LF}$	SO_3^{-1} ν_s, COC-A ν_{as}	983*	969
		COC-B ν_{as}, CF_3 δ_u, $SO_3^-\nu_s$	973*	983
	$C_{3v,HF}$	COC-A ν_{as}, SO_3^{-1} ν_s	1059*	1061
Dehydrated Nafion-[H]	$C_{1,LF}$	SO_3H ν_s, COC-A ν_s	786*	910
		CF_3 δ_u, COC-B ν_{as}	981*	983
	$C_{1,MF}$	CF_3 δ_u, COC-B δ_s, COC-A ρ_r, SO_3H ν_{as}	986*	999s
	$C_{1,HF}$	SO_3H ν_{as}, COC-A ν_{as}	1405*	1414
Hydrated 3M-[H]	$C_{3v,LF}$	SO_3^{-1} ν_s, COC ν_{as}	975*	991
		SO_3^{-1} ν_s, SC CC ν, COC δ_s	980*	1012
	$C_{3v,HF}$	SO_3^{-1} ν_s, COC ν_s	1014*	1060
Dehydrated 3M-[H]	$C_{1,LF}$	SO_3H ν_s, COC ν_s	791*	926
		COC ν_{as}	984*	1012
	$C_{1,MF}$	COC δ_s, SO_3H ν_{as}	1009*	1031
	$C_{1,HF}$	SO_3H ν_{as}	1395*	1412

Symmetric stretching, ν_s; Asymmetric stretching, ν_{as}; Wagging, ω; Bending, δ_s; Umbrella bending, δ_u; Rocking, ρ_r; Backbone, BB; Side Chain, SC; Calculated value *

Operando Raman Spectroscopy of the fuel cell ionomer/Pt interface of a non-PGM catalysts: A case study.

Ionomer vibrational band assignments in terms of exchange site local symmetry, and as group modes, are essential for the interpreting operando Raman spectroscopy of the fuel cell catalytic layer.

Operando confocal Raman micro-spectroscopy depth profiling to select focal point for fuel cell study.

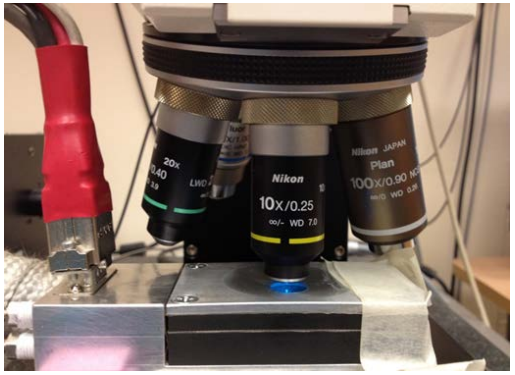

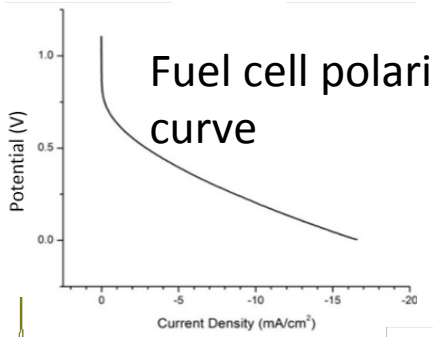

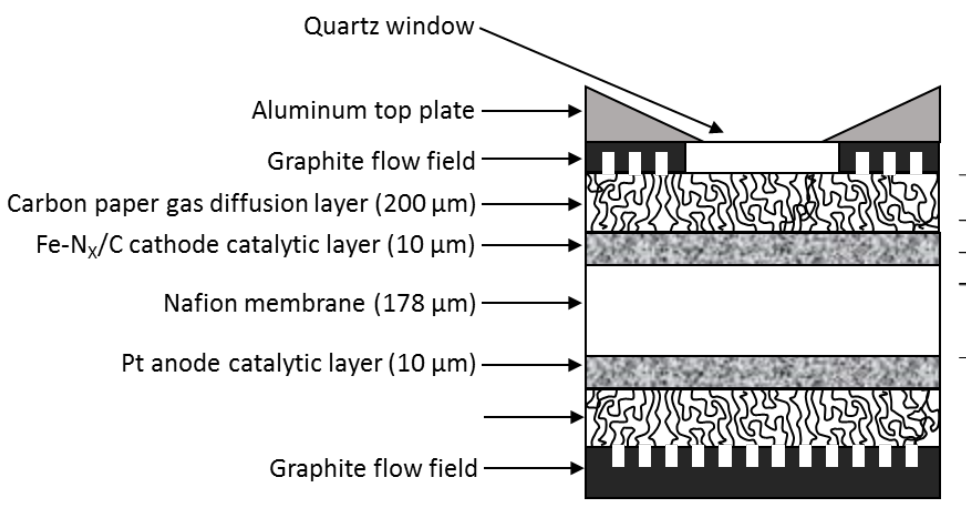

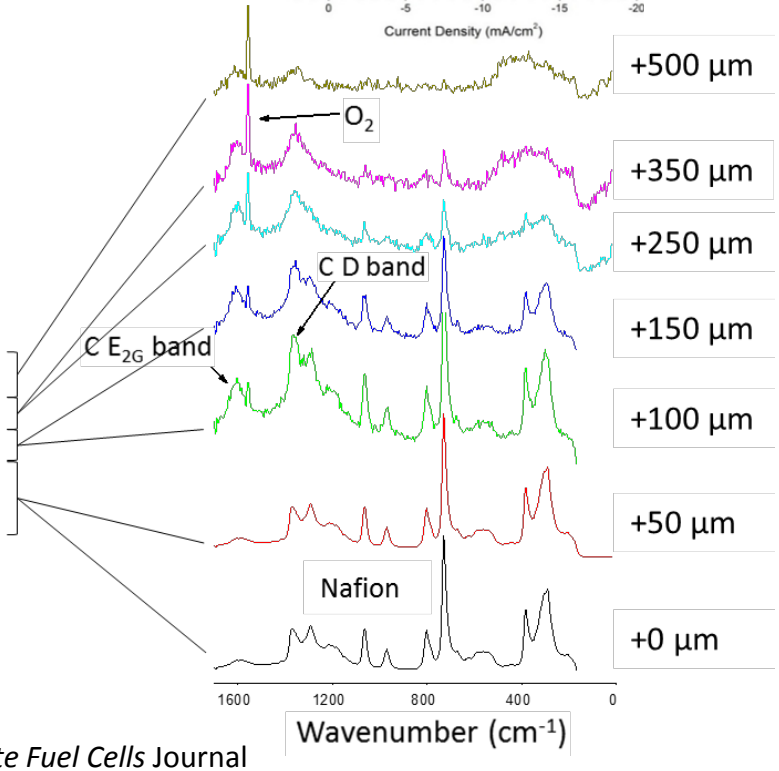

Kendrick et al. *Operando Raman Micro-Spectroscopy of Polymer Electrolyte Fuel Cells* Journal of The Electrochemical Society, 163 (4) H3152-H3159 (2016)
Loupe et al., *Twenty years of operando IR, X-ray absorption, and Raman spectroscopy: Direct methanol and hydrogen fuel cells,* Catalysis Today, In press, doi:10.1016/j.cattod.2016.06.012

Operando Raman Micro-Spectroscopy of PEM fuel cell.

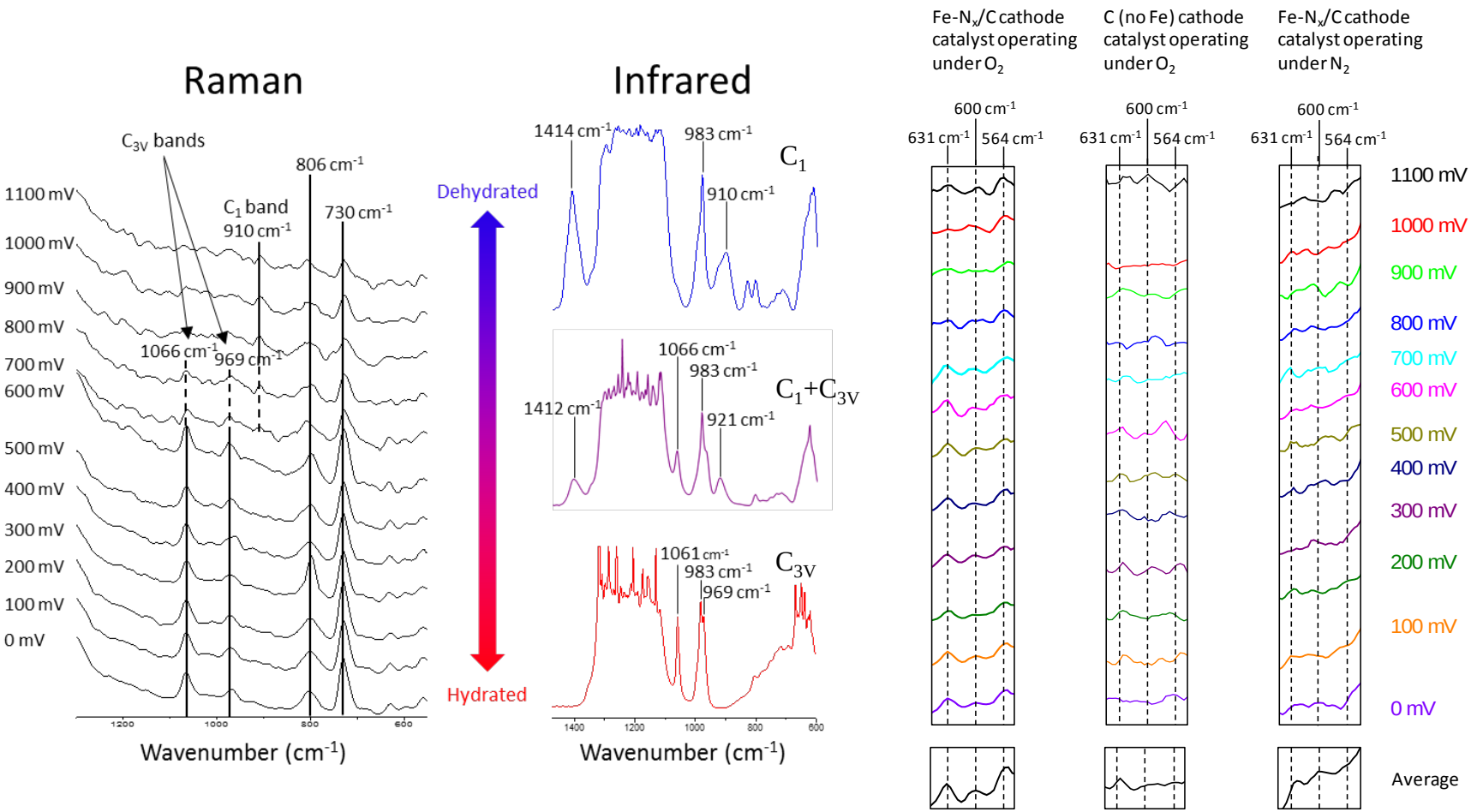

Kendrick Raman cell. Potential-dependent Raman spectra (650 to 550 cm^{-1}) of the Fe-Nx/C cathode catalyst operating under O_2 (left), under N_2 (middle), and under O_2 after Fe removal (right). Absence of Stark tuning of the Fe-O peak at 564 cm^{-1} confirms Fe-O is not an electrocatalytic site. Analysis of as-received catalyst showed 13.5 ppm Pt.

Conclusions

- This is the first demonstration of operando Raman spectroscopy of a fuel cell with flowing reactant streams over a standard MEA structure and controlled temperature.
- Stark tuning of the Fe-O site in a non-PGM catalyst was not observed in the operando Raman (i.e., Fe-O peaks were invariant with potential). Catalysis was likely due to Pt contaminant assessed at 13.5 ppm.
- Local symmetry based assignments of short chain, 3M and Nafion vibrational group modes (C_1 vs. C_{3V}) enables elucidation of shift of the λ per site distribution with state of hydration. This explains the gradual shift of ionomer spectra from C_1 to (C_1 + C_{3V}) to C_{3V} characteristics representing fully dehydrated, partially hydrated and totally hydrated exchange site environments respectively.

Thanks

Thanks to funding from:
NuVant Systems Inc.
US Department of Energy EERE (DE-EE-0000459)
Army Research Office (W911NF-12-1-0346)

Neili Loupe (NEU): Vibrational band assignments, and IR spectroscopy
Jonathan Doan (NEU): Vibrational band assignments and IR spectroscopy
Ryan Cruse (NEU): Per site λ analysis
Matthew Ingargiola (NEU): Per site λ analysis
Nicholas Dimakis (UT-RGV) : DFT Normal mode analysis
Khaldoon Abu-Hakmeh (Georgia Tech): MD simulations of λ = 3, 10 and 15
Seung Soon Jang (Georgia Tech): MD simulations of λ = 3, 10 and 15
Max Diem (NEU): Raman spectroscopy
Ian Kendrick (NEU): IR and Raman spectroscopy
William A. Goddard III (Cal Tech): MD simulations and use of his X3LYP functional for DFT build-up of hydration sphere.

Supplemental slides

The following slides are supplemental slides that were not shown at the CWG.

Short Side-Chain exchange-site normal modes

C_{3v} local symmetry

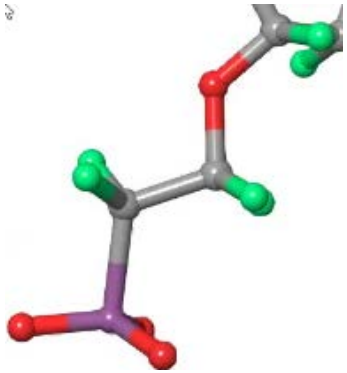

$C_{3v,LF}$

923* (970) cm^{-1} : SO_3^- v_s, COC v_{as}

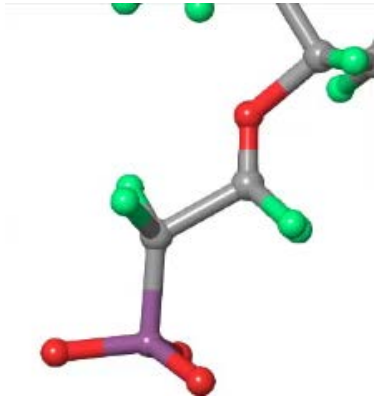

$C_{3v,HF}$

1051* (1057) cm^{-1} : COC v_{as}, SO_3^- v_s

C_1 local symmetry

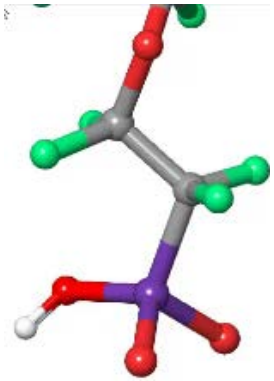

$C_{1,LF}$

777* (905) cm^{-1} : SO_3H v_s, COC v_s

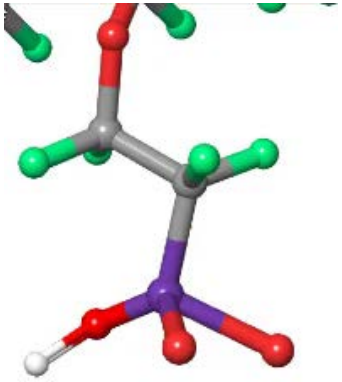

$C_{1,HF}$

1396* (1414) cm^{-1} : SO_3H v_{as}, COC v_{as}

3M PFSA exchange-site normal modes

C_{3v} local symmetry

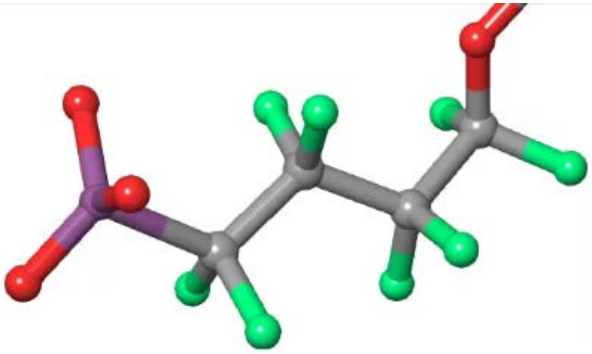

$C_{3v,LF}$

975* (991) cm^{-1} : SO_3^- v_s, COC v_{as}

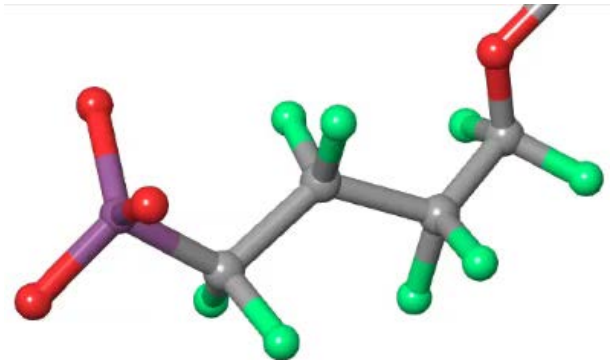

$C_{3v,HF}$

1014* (1060) cm^{-1} : SO_3^{-1} v_s, COC v_s

C_1 local symmetry

$C_{1,LF}$

791* (926) cm^{-1} : SO_3H v_s, COC v_s

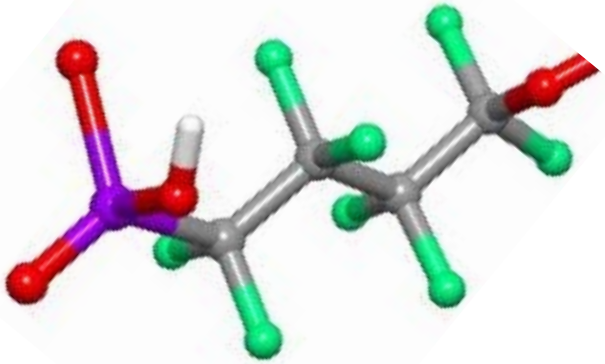

$C_{1,HF}$

1395* (1412) cm^{-1} : SO_3H v_{as}

Ley diagram

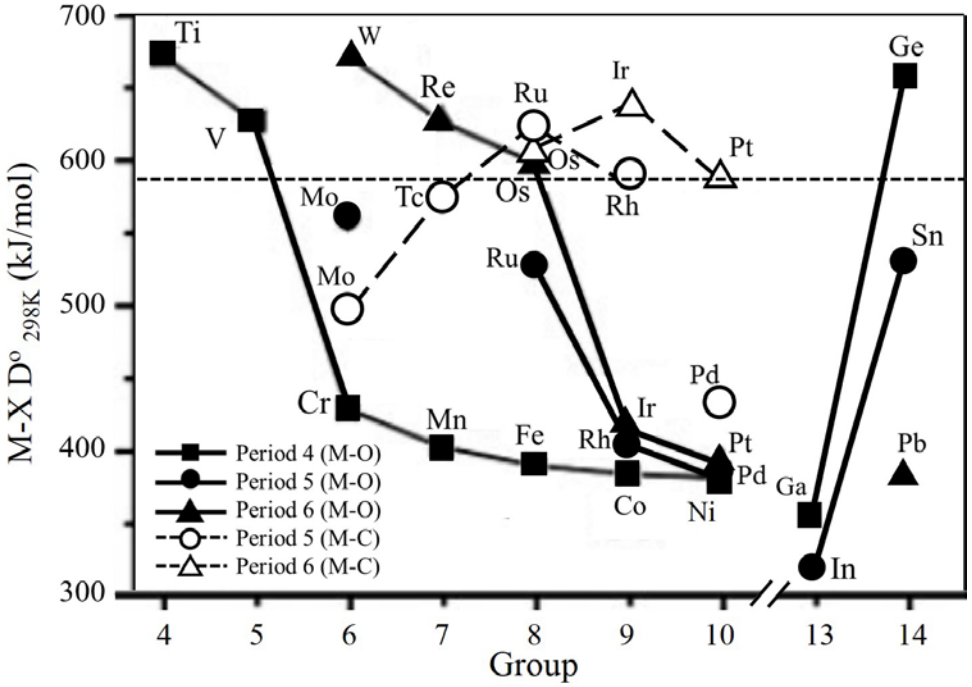

The metal-oxygen bond dissociation energy (D^o 298 K (M-O)) in diatomic molecules versus group. Periods are determined by symbols.

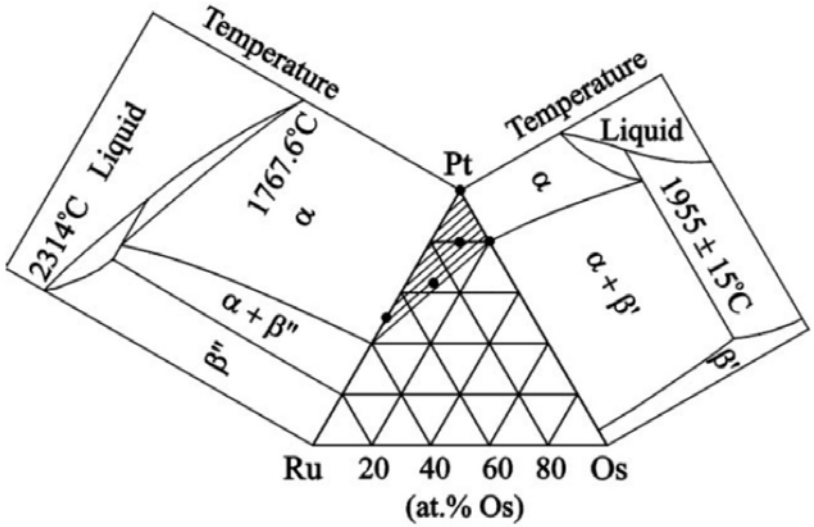

Face centered cubic (FCC) phase compositions in the PtRuOs system.

State-of-hydration dependent IR spectra